SCIENTIFIC REPORTS

OPEN

SUBJECT AREAS:
SUPERCONDUCTING PROPERTIES AND MATERIALS
FERROMAGNETISM

Received
8 October 2014

Accepted
3 December 2014

Published
13 January 2015

Correspondence and requests for materials should be addressed to T.M. (tomaz.mertelj@ijs.si)

Coexistence of ferromagnetism and superconductivity in iron based pnictides: a time resolved magnetooptical study

A. Pogrebna[1,2], T. Mertelj[1], N. Vujičić[1,3], G. Cao[4], Z. A. Xu[4] & D. Mihailovic[1,5]

[1]Complex Matter Dept., Jozef Stefan Institute, Jamova 39, SI-1000 Ljubljana, Slovenia, [2]Jožef Stefan International Postgraduate School, Jamova 39, SI-1000 Ljubljana, Slovenia, [3]Institute of Physics, Bijenička 46, HR-10000 Zagreb, Croatia, [4]Department of Physics, Zhejiang University, Hangzhou 310027, People's Republic of China, [5]CENN Nanocenter, Jamova 39, SI-1000 Ljubljana, Slovenia.

Ferromagnetism and superconductivity are antagonistic phenomena. Their coexistence implies either a modulated ferromagnetic order parameter on a lengthscale shorter than the superconducting coherence length or a weak exchange coupling between the itinerant superconducting electrons and the localized ordered spins. In some iron based pnictide superconductors the coexistence of ferromagnetism and superconductivity has been clearly demonstrated. The nature of the coexistence, however, remains elusive since no clear understanding of the spin structure in the superconducting state has been reached and the reports on the coupling strength are controversial. We show, by a direct optical pump-probe experiment, that the coupling is weak, since the transfer of the excess energy from the itinerant electrons to ordered localized spins is much slower than the electron-phonon relaxation, implying the coexistence without the short-lengthscale ferromagnetic order parameter modulation. Remarkably, the polarization analysis of the coherently excited spin wave response points towards a simple ferromagnetic ordering of spins with two distinct types of ferromagnetic domains.

In the iron-based superconductors family[1,2] $EuFe_2(As,P)_2$[3] and $Eu(Fe,Co)_2As_2$[4] offer an interesting experimental possibility to study the competition between the ferromagnetic (FM) and superconducting (SC) order parameters that can lead to nonuniform magnetic and SC states[4–7] since the optimal superconducting critical temperature $T_c \sim 28$ K[8] is comparable to the FM Eu^{2+}-spin ordering temperatures $T_C \sim 18$ K[3,9].

The strength and nature of the coupling between the carriers in the FeAs planes, responsible for superconductivity, and localized Eu^{2+} *f*-orbitals spins, responsible for ferromagnetism, is expected to influence strongly any possible magnetic as well as SC modulated state[6]. To enable coexistence of the singlet superconductivity with ferromagnetism in the case of strong exchange-interaction-dominated coupling the magnetization modulation period should be short on the lengthscale below the SC coherence length[5,6], which is a few[10,11] tens of nm in 122 iron based compounds. On the other hand, in the case of weaker long-range magnetic-dipole dominated coupling a longer lengthscale FM domain structure can effectively minimize the internal magnetic field enabling coexistence of the singlet superconductivity and FM state[12]. Alternatively a spontaneous SC vortex state[6] might form as proposed recently[13] for $EuFe_2(As,P)_2$.

In the literature opposing claims regarding the coupling between the carriers in the FeAs planes and localized Eu^{2+} spins exist. A weak coupling between Fe and Eu magnetic orders was initially suggested by Xiao *et al.*[14], while recently a strong coupling was suggested from the in-plane magnetoresistance[15] and NMR[16].

The strength of the coupling between the carriers in the FeAs planes and localized Eu^{2+} *f*-orbitals spins should be reflected also in the energy transfer speed between the two subsystems upon photoexcitation. We therefore systematically investigated the ultrafast transient reflectivity ($\Delta R/R$) dynamics and time resolved magneto-optical Kerr effect (TR-MOKE) in $EuFe_2(As_{1-x}P_x)_2$ in both, the undoped spin-density wave (SDW) and doped SC state. In addition to the relaxation components, that were observed earlier in related non-FM $Ba(Fe,Co)_2As_2$,[17,18] we found another slow-relaxation component associated with Eu^{2+}-magnetization dynamics. The relatively slow 0.1-1 nanosecond-timescale response of the Eu^{2+} spins to the optical excitation of the FeAs itinerant carriers

indicates a rather weak coupling between the two subsystems suggesting the magnetic-dipole dominated coupling between SC and FM order parameters.

Moreover, the antiferromagnetic (AFM) Eu^{2+}-spin order in the undoped SDW $EuFe_2As_2$, where the spins are aligned ferromagnetically in the *ab* plane with the A-type AFM order of the adjacent Eu^{2+} planes along the *c* axis, is rather well understood[9,14]. Contrary, no coherent picture of Eu^{2+}-spin ordering upon P or Co doping exists. In addition to the proposal of a SC induced helimagnetic ordering[4] in $Eu(Fe,Co)_2As_2$ a canted AFM was proposed by Zapf *et al.*[19] in superconducting $EuFe_2(As_{1-x}P_x)_2$, while a pure FM ordering[13] at $x = 0.15$ coexisting with superconductivity was reported by Nandi *et al.*[13]. A spin-glass state over the all P doping range was also suggested by Zapf *et al.*[20] recently.

The observed time-resolved magnetooptical transients in the presence of an in-plane magnetic field reveal an additional coherent magnon response in the superconducting sample. The polarization dependence of the coherent magnon oscillations *points towards a FM domain state* consistent with results of Nandi *et al.*[13].

Results

Temperature dependence of photoinduced reflectivity. In Fig. 1 a)–d) we show temperature dependence of the transient reflectivity ($\Delta R/R$) measured with the probe pulses polarized in the *ab*-plane in undoped nonsuperconducting $EuFe_2As_2$ (Eu-122) and doped superconducting $EuFe_2(As_{0.81}P_{0.19})_2$ (EuP-122). The transient reflectivity is anisotropic in the *ab*-plane, consistent with the orthorhombic crystal structure. We indicate the two orthogonal polarizations $\mathcal{P}^+$ and $\mathcal{P}^-$ according to the sign of the subpicosecond transient reflectivity. In addition to the anisotropic fast component associated with the SDW order discussed elsewhere[21] we observe in both samples, concurrently with emergence of the Eu^{2+}-spin ordering[14,19], appearance of another much slower relaxation component with a risetime of $\sim$ 1 ns in Eu-122 and $\sim$ 100 ps in EuP-122 (at $T = 1.5$ K) and the decay time beyond the experimental delay range. The amplitude, *A*, of the slow component, corresponding to the long-delay extremum of $\Delta R/R$ shown in Fig. 2 is clearly correlated with the Eu^{2+} magnetic moment. In the vicinity of the Eu^{2+} magnetic ordering temperature a marked increase of the risetime is observed in both samples. In Eu-122 the slow component is rather anisotropic, while in EuP-122 it appears almost isotropic.

The probe-photon-energy dependence of the transients in Eu-122 is shown in Fig. 3. The dispersion of the fast component[21] is much broader than that of the slow one, which shows a relatively narrow resonance around $\sim$1.7 eV.

Metamagnetic transitions. Upon application of magnetic field lying in the *ab*-plane the Eu^{2+} AFM order in Eu-122 is destroyed above $\mu_0 H \sim 0.8$ T in favor of an in-plane field-aligned FM state[22–24]. In EuP-122 a similar field-induced spin reorientation from the out-of-plane FM into the in-plane field-aligned FM state was observed around $\mu_0 H \sim 0.6$ T[13]. These metamagnetic transitions have remarkable influence on the transient reflectivity as shown in Fig. 4. While the fast picosecond response associated with the SDW state[21] shows virtually no dependence on the magnetic field, the slow response shows a marked change in the field-induced FM state[13,22–24].

In undoped Eu-122 the $\mathcal{P}^+$-polarization slow response is suppressed above the metamagnetic transition [Fig. 4 (a)] and is magnetic-field independent above 2 T. Concurrently, for the $\mathcal{P}^-$ polarization, which is parallel to the magnetic field, [Fig. 4 (b)] the slow response is first enhanced at low magnetic field above the transition, resembling a rotation of the anisotropy by $\pi/2$, and then slightly suppressed upon increasing the field to 7 T.

In EuP-122 the initially positive rather isotropic slow response [Fig. 4 (c), (d)] switches to a negative anisotropic one along the $\mathcal{P}^+$ polarization, parallel to the magnetic field. Similar to Eu-122 the slow response is slightly suppressed at the highest field with a faster relaxation.

Coherent spin waves. In EuP-122 at low magnetic fields below $\sim$ 0.5 T additional damped oscillations appear on top of the slow relaxation in $\Delta R/R$ [see Fig. 5 (a), (b)]. These oscillations appear rather isotropic. The amplitude of the oscillations, shown in Fig. 6 (d), is strongly peaked around $\sim$ 0.25 T and vanishes at 0.5 T. The

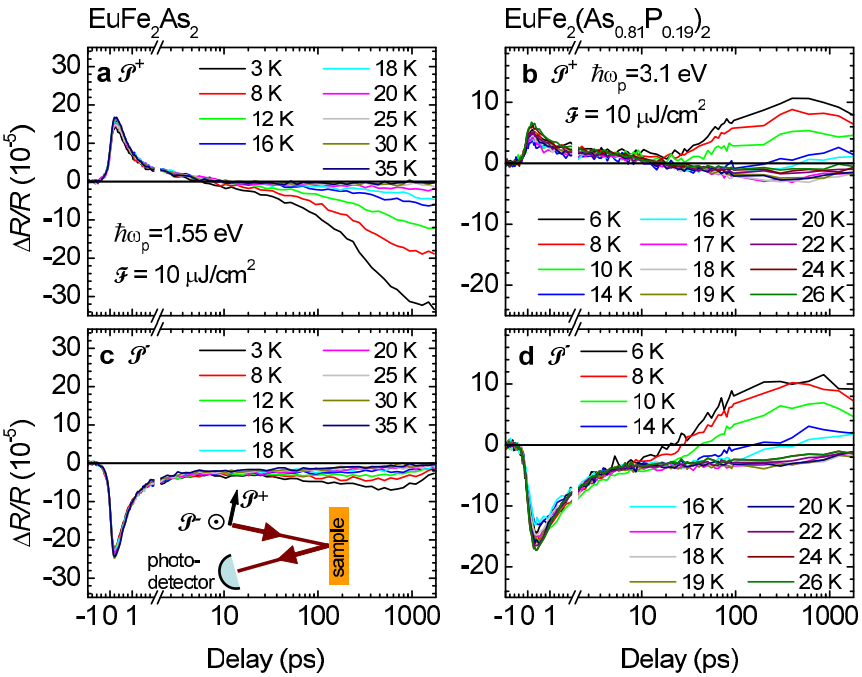

Figure 1 | Temperature dependence of the *ab*-plane transient reflectivity. Photoinduced reflectivity transients at low-*T* in $EuFe_2As_2$ (a), (c) and $EuFe_2(As_{0.81}P_{0.19})_2$ (b), (d) for two probe-photon polarizations. Inset to (c) represents a schematic of the probe beam configuration. $\mathcal{P}^+$ and $\mathcal{P}^-$ correspond to two orthogonal in-plane probe-photon polarizations.

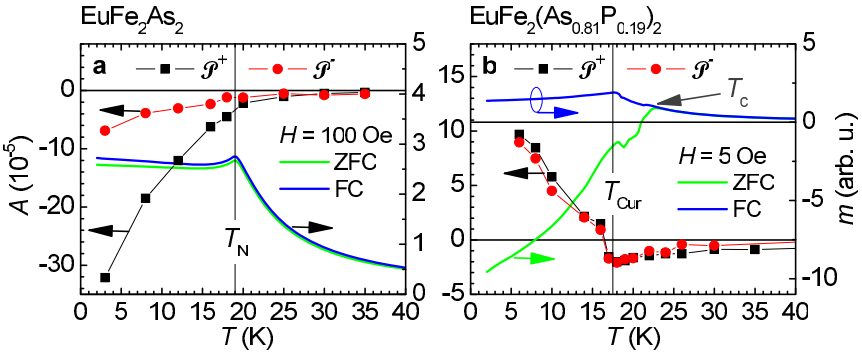

Figure 2 | Temperature dependence of the slow transient-reflectivity component amplitude. The amplitude of the photoinduced reflectivity transients at long delays as a function of temperature in $EuFe_2As_2$, (a), and $EuFe_2(As_{0.81}P_{0.19})_2$, (b), compared to the magnetic moment along the *c*-axis. $\mathcal{P}^+$ and $\mathcal{P}^-$ correspond to two orthogonal in-plane probe-photon polarizations while ZFC and FC correspond to cooling in the presence and absence of magnetic field, respectively.

frequency of the oscillations, as determined by a damped oscillator fit, $\Delta R_{osc}/R = A_{osc}\exp(-t/\tau)\cos(\omega_0 t)$, shown in Fig. 6 (a), is H independent at low fields and starts to decrease with increasing field above $\mu_0 H \sim 0.3$ T. The damping, on the other hand, is magnetic-field independent at $\tau^{-1} \sim 10$ GHz.

Another oscillation with a higher frequency (~ 14.5 GHz at 0.3 T) is revealed by the transient magnetooptical Kerr effect (TR-MOKE) shown in Fig. 5 (c)–(f). The oscillatory part of the transient rotation and ellipticity is polarization independent and almost even with respect to the reversal of magnetic field.

Discussion

Eu^{2+} ions have [Xe]$4f^7 6s^2$ ($^8S_{7/2}$) electronic configuration. The lowest excited states of a free Eu^{2+} ion are ~ 3.5 eV above the ground state[26]. In oxides, however, this splitting can be reduced down to ~ 1 eV[26,27]. In Eu-122 the position of *f*-derived states was calculated to be ~ 2 eV below the Fermi energy[28], close to the observed Eu^{2+}-spin ordering related slow-component resonance around 1.7 eV [see Fig. 3 (b)]. It is therefore plausible that the coupling of the Eu^{2+} magnetism to the dielectric constant at the probe photon energy of 1.55 eV is through the resonant magneto-optical Cotton-Mouton effect with the location of the Eu^{2+}-4*f* states ~ 1.7 eV below the Fermi level.

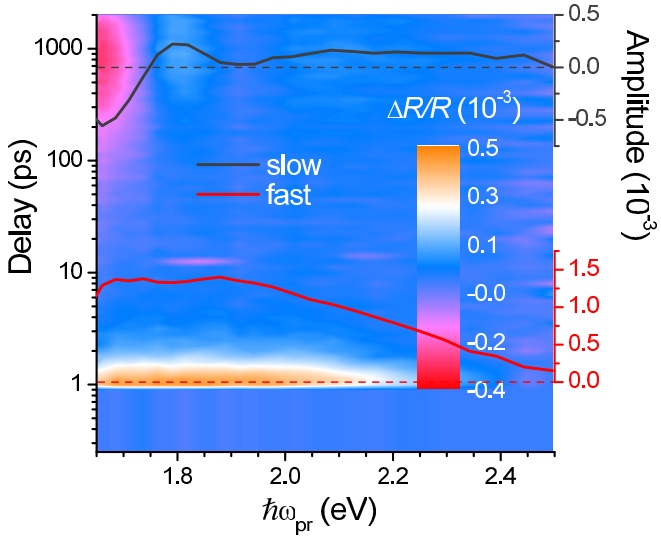

Figure 3 | Photoinduced reflectivity transients at low-*T* in $EuFe_2As_2$ as a function of probe photon energy for the $\mathcal{P}^+$ polarization. The spectral dependencies of the fast and slow response amplitude are shown as red and dark-grey lines, respectively.

On the other hand, a large magnetostriction is indicated from the realignment of the crystal twin domain structure in magnetic field[23], suggesting a possibility of the indirect contribution to the optical dielectric function through the magnetoelastic effect. The rather narrow probe-photon-energy resonance of the slow component does not support this mechanism.

We should also note that the realignment of the twin domain structure[23] was not observed in our experiment, since the anisotropy of the fast component, which is associated with the structural twin domains[18], shows no dependence on magnetic field in both samples (see Fig. 4) up to $\mu_0 H = 7$ T. Moreover, the realignment of the twin domain structure observed in Ref. 23 might be related to the Fe spin ordering as indicated by observation of a partial magnetic field detwinning also in non-ferromagnetic $Ba(Fe_{1-x}Co_x)_2As_2$[29].

The strong in-plane anisotropy of the slow component in Eu-122 indicates that the response corresponds to the dynamics of the in-plane component of the sublattice Eu^{2+} magnetizations. The presence of qualitatively same response in the in-plane field-aligned FM state suggests that the observed slow dynamics is not dominated by the orientational dynamics of the AFM sublattice magnetizations, but rather by the longitudinal dynamics of the individual sublattice magnetizations. The response can therefore be associated with a decrease of the Eu^{2+} magnetization upon photoexcitation in both, the zero-field AFM and the field-induced in-plane FM state.

To understand the change of the anisotropy between weak and strong magnetic fields in EuP-122 let us look at the symmetric part of the in-plane dielectric tensor components ϵ_{ii}. Within the orthorhombic point symmetry ϵ_{ii} can be expanded in terms of magnetization to the lowest order as:

$$\epsilon_{ii} = \epsilon_{0,ii} + a_{iizz}M_z^2 + a_{iixx}M_x^2 + a_{iiyy}M_y^2, \qquad (1)$$

with $i \in \{x, y\}$. Here **M** would correspond to the Eu^{2+} sublattice magnetization in the case of a canted AFM ordering, or the total Eu^{2+} magnetization in the case of FM ordering. In EuP-122 in low magnetic fields **M** is predominantly oriented along the *c*-axis[13,30] leading to the nearly isotropic response, since $a_{xxzz} \sim a_{yyzz}$ due to the small orthorhombic lattice distortion. In the field-induced FM state and the zero-field AFM state of Eu-122 **M** lies in the *ab*-plane leading to an anisotropic response since it is quite unlikely that $a_{iiii} \sim a_{jjii}$, with $i \neq j$.

The photoinduced Eu^{2+} demagnetization is therefore slow, on a nanosecond timescale in Eu-122 and a ~ 100 ps timescale in EuP-122. It can not be due to a direct emission of incoherent Eu^{2+} magnons by the eV-energy photoexcited Fe-*d*-bands electron-hole pairs since it has been shown, that in the case of iron-based pnictides in the SDW state the Fe-*d*-bands quasiparticle relaxation occurs on a picosecond timescale[21,31,32] and goes through emission of Fe-*d*-spin

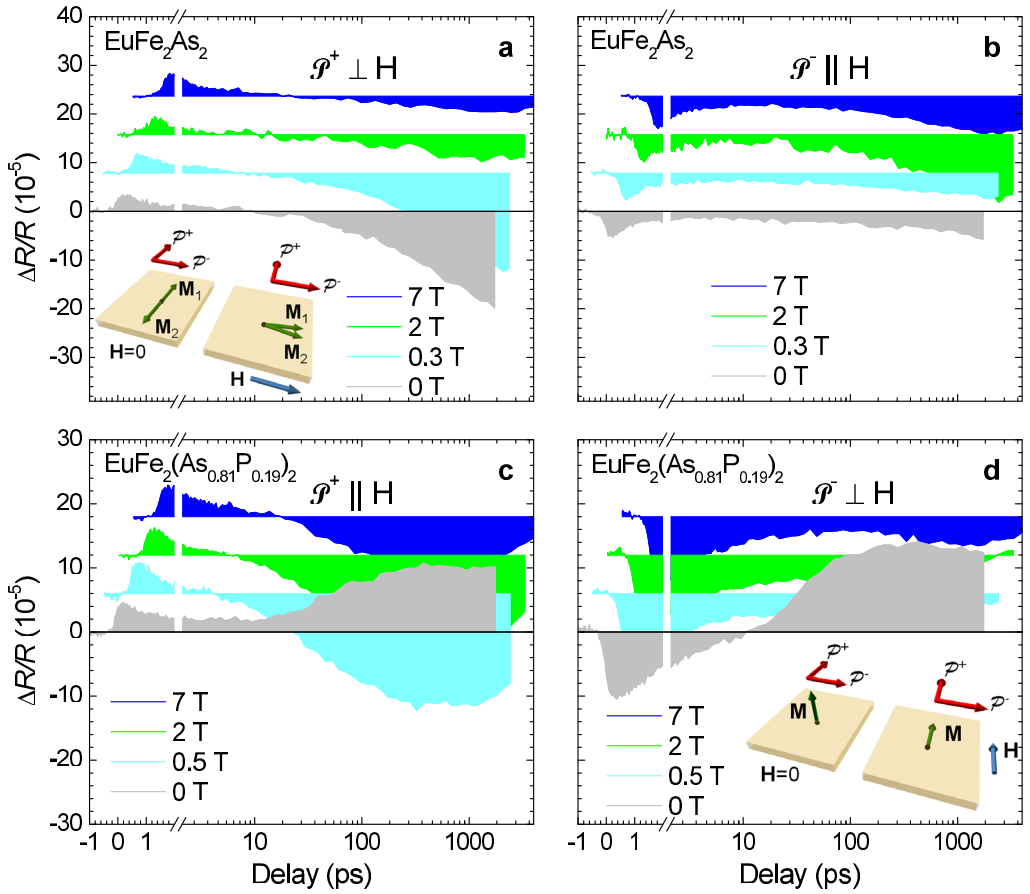

Figure 4 | In-plane magnetic field dependence of the transient reflectivity. (a), (b) The reflectivity transients in $EuFe_2As_2$ with the magnetic field parallel to the $\mathcal{P}^-$ polarization. (c), (d) The reflectivity transients in $EuFe_2(As_{0.81}P_{0.19})_2$ with the magnetic field field paralel to the $\mathcal{P}^+$ polarization. All transient were measured at $T = 2$ K, $\mathcal{F} \sim 3\ \mu J/cm^2$ and 1.55-eV pump-photon energy. Insets show shematically magnetization reorientation in magnetic field.

magnons[21] followed by relaxation to phonons. It can therefore be assumed that the Fe-*d*-bands quasiparticle and lattice degrees of freedom are fully thermalized beyond ~ 10 ps when the slow component starts to emerge. This suggests that *the energy transfer from the excited quasiparticles in the Fe-d bands to the* Eu^{2+} *magnons is rather inefficient*. The incoherent Eu^{2+} magnons are therefore excited indirectly via the spin-lattice coupling only after the initial excitation energy was thermally distributed between the Fe-*d*-bands quasiparticles and phonons. *The* Eu^{2+} *spins therefore appear only weakly coupled to the Fe-d-bands quasiparticles with the coupling increasing with the P doping*. The rather large in-plane magnetoresistance observed by Xiao *et al.*[15] in Eu-122 can therefore be attributed to slow magnetostriction effects modifying the lattice twin domain structure.

The light penetration depth at the probe-photon energy of $\hbar\omega_{pr} =$ 1.55 eV is ~ 27 nm[33], while the beam diameters are in a 100 μm range. Irrespective of the excitation mechanism, which can be either nonthermal impulsive[34] inverse Cotton-Mouton effect or thermal displacive non-Raman[35] like, it can be assumed that the relevant wavevectors are $q \lesssim 1/30\ nm^{-1}$ and dominantly a uniform coherent magnetization precession is excited and detected. (In the case of helical magnetic order with the propagation vector $\mathbf{q}_0$, spin waves at $\mathbf{q} = \pm m\mathbf{q}_0$, $m \in \mathbb{Z}$, also need to be considered[36].)

The low frequency mode observed in the transient reflectivity response softens with increasing temperature and vanishes in the field induced in-plane FM state so it can definitely be assigned to a magnetic mode. The high frequency mode has also a magnetic origin since it appears in the TR-MOKE configuration only.

Analyzing contributions of the magnetization displacements, δM_i, to the symmetric part of the optical response it follows from (1),

$$\delta\epsilon_{ii} = 2a_{iizz}M_z\delta M_z + 2a_{iixx}M_x\delta M_x + 2a_{iiyy}M_y\delta M_y. \qquad (2)$$

The low-frequency mode is very strong in $\Delta R/R$ and rather isotropic in the *ab*-plane indicating that is either associated with the out of-plane terms (i) $2a_{iizz}M_z\delta M_z$ or (ii) both, M_x and M_y, are finite such as in the case of a helimagnetic ordering. In the latter case the local magnetization needs to be considered since the average of the terms $<M_i\delta M_i>$, $i \in \{x, y\}$, over Eu^{2+} planes is finite despite $<M_i> = 0$. Concurrently, it is weak in the TR-MOKE configuration, which is sensitive to δM_z. Since $\delta M_z \neq 0$ for both (i) and (ii) (see Supplemental information for case (ii)) this indicates that the measured volume is composed from the "up" and "down" magnetic domains magnetized along the *c*-axis. The sign of δM_z varies in different magnetic domains leading to a vanishing TR-MOKE response averaged over many magnetic domains, while the sign of $M_z\delta M_z$ does not depend on the domain orientation and averages to a finite value.

For the high-frequency mode observed in the TR-MOKE configuration, on the other hand, the averaged δM_z is finite while the averaged $M_z\delta M_z$ is rather small in comparison to the low frequency mode. This indicates that in addition to the *c*-axis magnetized domains in-plane magnetized regions exist with $M_z \sim 0$. The in-plane magnetization leads to an out of plane magnetization displacement with $\delta M_z \neq 0$ and $M_z\delta M_z \sim 0$, consistent with the observed magnetic field dependence of the mode frequency. The invariance of the oscillatory TR-MOKE response [see. Fig. 5 (c)–(f)] with respect

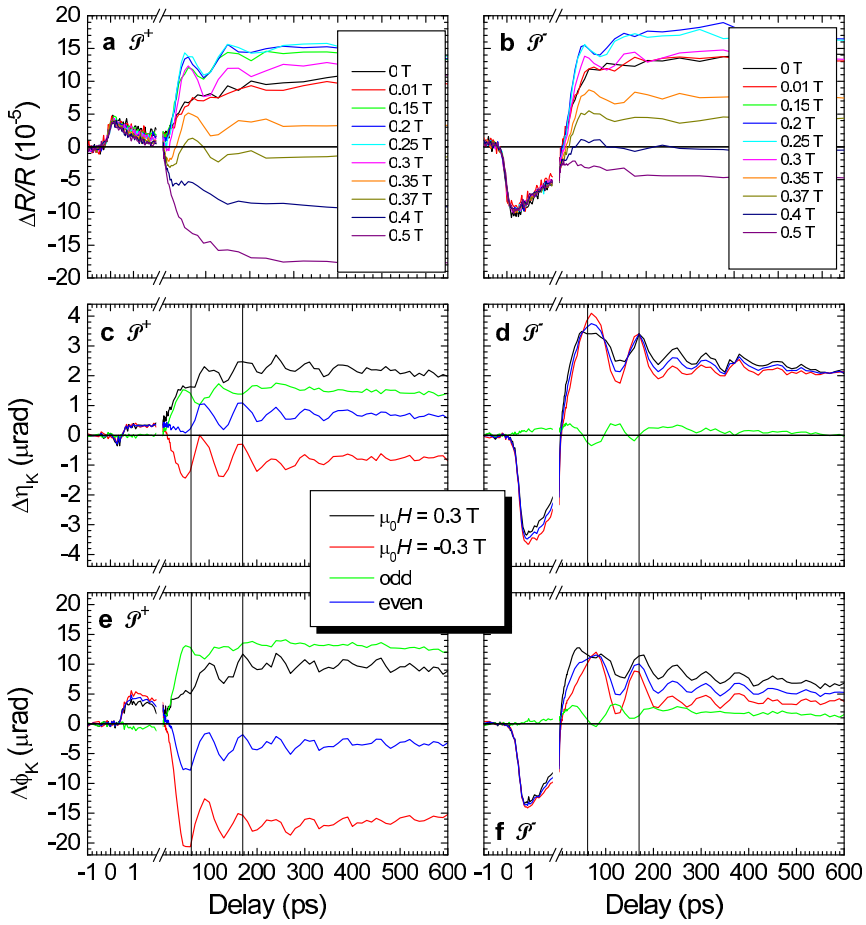

Figure 5 | (a), (b) The reflectivity transients in $EuFe_2(As_{0.81}P_{0.19})_2$ in low magnetic fields at $T = 2$ K, $\mathcal{F} = 3$ $\mu J/cm^2$ and 1.55-eV pump photon energy. Transient Kerr ellipticity, (c), (d), and rotation, (e), (f), upon reversal of the magnetic field at $T = 1.5$ K and $\mathcal{F} = 10$ $\mu J/cm^2$. Odd and even part of the responses correspond to the difference an the sum of the responses measured at different signs of the magnetic field, respectively.

to the inversion of the magnetic field is also consistent with the in-plane magnetization orientation.

A fit of the frequency magnetic-field dependence [see Fig. 6 (b)] using the standard uniaxial ferromagnet formula for a parallel magnetic field[25] ignoring demagnetization factors, $\omega = \gamma_{ab}(H_{ab} + H)$, yields $\mu_0 H_{ab} = 0.3$ T and $\gamma_{ab}/\mu_0 = 182$ GHz/T. The obtained gyromagnetic ratio $g_{ab} = 2.06$ is consistent with $^8S_{7/2}$ state of Eu^{2+} ions. The absence of demagnetization factors suggests that the response does not originate from the domain walls between the *c*-axis oriented domains but rather from planar shaped domains. Due to surface sensitivity (~ 30 nm) of the optical probe these are very likely surface domains, however, the bulk nature of these domains can not be entirely excluded.

The observed behaviour is compatible with the simple ferromagnetic order (within the domains) proposed by Nandi *et al.*[13]. In the absence of the in-plane magnetic field the static magnetization in the *c*-axis domains is along the *c*-axis and $\delta M_z = 0$, consistent with the vanishing amplitude of the low frequency mode near the zero field. Upon application of the in-plane magnetic field the magnetization is tilted away from the *c*-axis (see inset to Fig. 6) leading to a finite δM_z and the observed decrease of the mode frequency[25]. The decrease of the transient-reflectivity amplitude, when approaching to the metamagnetic transition, can be associated with the vanishing M_z.

A fit of the frequency magnetic-field dependence using the standard uniaxial ferromagnet formula for the perpendicular magnetic field[25] ignoring demagnetization factors, $\omega = \gamma_c\sqrt{H_c^2 - H^2}$, results in $\mu_0 H_c = 0.52$ T and $\gamma_c/\mu_0 = 119$ GHz/T. The small value of γ_c leading to a small gyromagnetic ratio ($g_c = 1.35$) can be attributed to the ignored unknown demagnetization factors of the *c*-axis magnetized domains. Moreover, it suggests that the *c*-axis magnetized domains have a flat shape with the normal perpendicular to the *c* axis.

On the other hand, the presence of two distinct modes and the magnetic field dependence of the mode frequencies [see Fig. 6 (b)] resembles the standard uniaxial AFM cases with the magnetic field perpendicular to the easy/hard axis[25,37] indicating a possible canted AFM[19] (CAFM) order. The polarization dependence of the modes is, however, *not compatible* with the CAFM picture since both, the quasi-AFM mode[38] and the quasi-FM mode, contribute to δM_z (see Supplemental) and should, contrary to the observations, contribute concurrently to the transient reflectivity and the TR-MOKE with identical relative amplitudes.

In the case of the conical helimagnetic ordering[4,30,39] the in-plane isotropy naturally appears for certain modes (see Supplemental). However, since, as in the case of the CAFM state, contributions of more than one magnetic mode to δM_z are expected, our data do not support the conical helimagnetic ordering.

In conclusion, our data point towards the simple FM Eu^{2+}-spin order in superconducting $EuFe_2(As,P)_2$ proposed by Nandi *et al.*[13]. The observed weak coupling between the FeAs-plane quasiparticles and Eu^{2+} spins indicates a weak magnetic-dipole dominated coupling between the SC and FM order parameters. This indicates that the coexistence of the singlet superconductivity with ferromagnetism in $EuFe_2(As_{1-x}P_x)_2$ is possible without necessity of the magnetic structure modulation on the lengthscale shorter than the SC coherence-length. The presence of the FM domain structure on longer

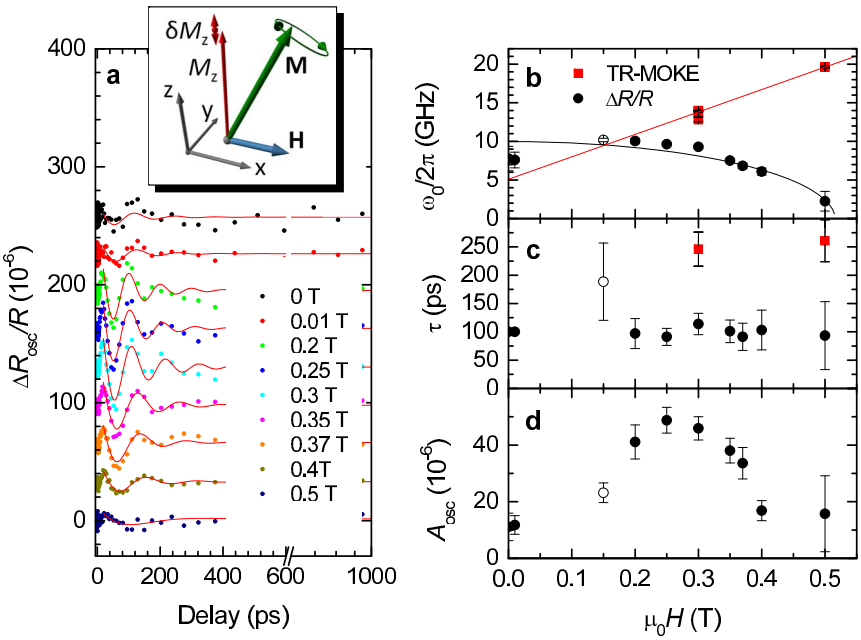

Figure 6 | (a) The oscillatory part of the isotropic $\Delta R/R$ component in $EuFe_2(As_{0.81}P_{0.19})_2$ at low magnetic fields, $\mathcal{F} = 3\ \mu J/cm^2$ and 1.5-eV pump photon energy. Thin lines represent the damped oscillator fits discussed in text. The frequency (b), decay time (c) and amplitude (e) of the oscillations as functions of the magnetic field. The points (open symbols) at $B = 0.15$ T were obtained from the $\mathcal{P}^-$ polarization fit due to the lack of data at the $\mathcal{P}^+$ polarization. The red squares were obtained from TR-MOKE fits. The lines in (b) are uniaxial ferromagnet[25] fits discussed in text. The inset to (a) schematically shows magnetization precession in small magnetic fields with corresponding projections onto the *z*-axis.

lengthscales, which is inferred from the coherent-spin-wave response, might additionally contribute to stability of the coexisting state.

Methods

Sample preparation. Single crystals of $EuFe_2(As_{1-x}P_x)_2$ were grown by a flux method, similar to a previous reports[21,40] The out-of-plane magnetic susceptibilities shown in Fig. 1 are consistent with previous results[20,22]. From the susceptibility we infer Eu^{2+} spin ordering temperatures $T_N = 19$ K and $T_{Cur} = 17.6$ K in $EuFe_2As_2$ (Eu-122) and $EuFe_2(As_{0.81}P_{0.19})_2$ (EuP-122), respectively. EuP-122 also shows the onset of superconductivity at $T_c = 22.7$ K.

Optical measurements. Measurements of the photoinduced transient reflectivity, $\Delta R/R$, from *ab* facets of freshly cleaved samples at nearly normal incidence were performed using a standard pump-probe technique, with 50 fs optical pulses from a 250-kHz Ti:Al_2O_3 regenerative amplifier seeded with an Ti:Al_2O_3 oscillator[18]. We used the pump photons with both, the laser fundamental ($\hbar\omega_P = 1.55$ eV) and the doubled ($\hbar\omega_P = 3.1$ eV) photon energy, and the probe photons with the laser fundamental ($\hbar\omega_{pr} = 1.55$ eV) photon energy.

Magnetooptical measurements. Transient Kerr rotation, $\Delta\phi_K$, was also measured on *ab* facets of freshly cleaved samples at nearly normal incidence by means of a balanced detector scheme using a Wollaston prism and a standard homodyne modulation technique in a 7-T split-coil optical superconducting magnet. To measure the transient Kerr ellipticity, $\Delta\eta_K$, a $\pi/4$-waveplate was inserted in front of the Wollaston prism. In order to minimize the pollution of the Kerr signals with the photoinduced reflectivity signal the detector was carefully balanced prior to each scan.

1. Kamihara, Y. *et al.* Iron-based layered superconductor: LaOFeP. *Journal of the American Chemical Society* **128**, 10012–10013 (2006).
2. Kamihara, Y., Watanabe, T., Hirano, M. & Hosono, H. Iron-Based Layered Superconductor $La[O_{1-x}F_x]FeAs$ ($x = 0.05 - 0.12$) with $T_c = 26$ K. *J. Am. Chem. Soc* **130**, 3296–3297 (2008).
3. Ren, Z. *et al.* Superconductivity induced by phosphorus doping and its coexistence with ferromagnetism in $EuFe_2(As_{0.7}P_{0.3})_2$. *Physical Review Letters* **102**, 137002 (2009).
4. Jiang, S. *et al.* Superconductivity and local-moment magnetism in $Eu(Fe_{0.89}Co_{0.11})_2As_2$. *Phys. Rev. B* **80**, 184514 (2009).
5. Anderson, P. W. & Suhl, H. Spin alignment in the superconducting state. *Phys. Rev.* **116**, 898–900 (1959).
6. Buzdin, A. I., Bulaevskiĭ, L. N., Kulich, M. L. & Panyukov, S. V. Magnetic superconductors. *Soviet Physics Uspekhi* **27**, 927–935 (1984).
7. Błachowski, A. *et al.* Interplay between magnetism and superconductivity in $EuFe_{2-x}Co_xAs_2$ studied by ^{57}Fe and ^{151}Eu Mossbauer spectroscopy. *Phys. Rev. B* **84**, 174503 (2011).
8. Jeevan, H. S., Kasinathan, D., Rosner, H. & Gegenwart, P. Interplay of antiferromagnetism, ferromagnetism, and superconductivity in single crystals $EuFe_2(As_{1-x}P_x)_2$. *Phys. Rev. B* **83**, 054511 (2011).
9. Ren, Z. *et al.* Antiferromagnetic transition in $EuFe_2As_2$: a possible parent compound for superconductors. *Physical Review B* **78**, 052501 (2008).
10. Yin, Y. *et al.* Scanning tunneling spectroscopy and vortex imaging in the iron pnictide superconductor $BaFe_{1.8}Co_{0.2}As_2$. *Phys. Rev. Lett.* **102**, 097002 (2009).
11. Shan, L. *et al.* Observation of ordered vortices with andreev bound states in $Ba_{0.6}K_{0.4}Fe_2As_2$. *Nature Physics* **7**, 325–331 (2011).
12. Fauré, M. & Buzdin, A. I. Domain structure in a superconducting ferromagnet. *Phys. Rev. Lett.* **94**, 187202 (2005).
13. Nandi, S. *et al.* Coexistence of superconductivity and ferromagnetism in P-doped $EuFe_2As_2$. *Phys. Rev. B* **89**, 014512 (2014).
14. Xiao, Y. *et al.* Magnetic structure of $EuFe_2As_2$ determined by single-crystal neutron diffraction. *Physical Review B* **80**, 174424 (2009).
15. Xiao, Y. *et al.* Anomalous in-plane magnetoresistance in a $EuFe_2As_2$ single crystal: Evidence of strong spin-charge-lattice coupling. *Phys. Rev. B* **85**, 094504 (2012).
16. Guguchia, Z. *et al.* Strong coupling between Eu^{2+} spins and Fe_2As_2 layers in $EuFe_{1.9}Co_{0.1}As_2$ observed with NMR. *Physical Review B* **83**, 144516 (2011).
17. Torchinsky, D. H. *et al.* Nonequilibrium quasiparticle relaxation dynamics in single crystals of hole- and electron-doped $BaFe_2As_2$. *Phys. Rev. B* **84**, 104518 (2011).
18. Stojchevska, L., Mertelj, T., Chu, J., Fisher, I. & Mihailovic, D. Doping dependence of femtosecond quasiparticle relaxation dynamics in Ba(Fe, Co)$_2As_2$ single crystals: Evidence for normal-state nematic fluctuations. *Physical Review B* **86**, 024519 (2012).
19. Zapf, S. *et al.* Varying Eu^{2+} magnetic order by chemical pressure in $EuFe_2(As_{1-x}P_x)_2$. *Phys. Rev. B* **84**, 140503 (2011).
20. Zapf, S. *et al.* $EuFe_2(As_{1-x}P_x)_2$: Reentrant spin glass and superconductivity. *Physical Review Letters* **110**, 237002 (2013).
21. Pogrebna, A. *et al.* Spectrally resolved femtosecond reflectivity relaxation dynamics in undoped spin-density wave 122-structure iron-based pnictides. *Phys. Rev. B* **89**, 165131 (2014).
22. Jiang, S. *et al.* Metamagnetic transition in $EuFe_2As_2$ single crystals. *New Journal of Physics* **11**, 025007 (2009).
23. Xiao, Y. *et al.* Field-induced spin reorientation and giant spin-lattice coupling in $EuFe_2As_2$. *Physical Review B* **81**, 220406 (2010).
24. Guguchia, Z. *et al.* Anisotropic magnetic order of the Eu sublattice in single crystals of $EuFe_{2-x}Co_xAs_2$ ($x = 0, 0.2$) studied by means of magnetization and magnetic torque. *Phys. Rev. B* **84**, 144506 (2011).
25. Turov, E. A., Tybulewicz, A. & Chomet, S. *Physical properties of magnetically ordered crystals* (Academic Press, New York and London, 1965).

26. Dorenbos, P. Energy of the first $^4f_7 \rightarrow {}^4f_6$ 5*d* transition of Eu^{2+} in inorganic compounds. *Journal of Luminescence* **104**, 239–260 (2003).
27. Feinleib, J. *et al.* Spin-polarized splittings in the temperature-dependent reflectance of EuO. *Physical Review Letters* **22**, 1385 (1969).
28. Li, W., Zhu, J.-X., Chen, Y. & Ting, C. S. First-principles calculations of the electronic structure of iron-pnictide $EuFe_2(As,P)_2$ superconductors: Evidence for antiferromagnetic spin order. *Phys. Rev. B* **86**, 155119 (2012).
29. Chu, J.-H. *et al.* In-plane electronic anisotropy in underdoped $Ba(Fe_{1-x}Co_x)_2As_2$ revealed by partial detwinning in a magnetic field. *Phys. Rev. B* **81**, 214502 (2010).
30. Nowik, I., Felner, I., Ren, Z., Cao, G. H. & Xu, Z. A. Coexistence of ferromagnetism and superconductivity: magnetization and Mössbauer studies of $EuFe_2(As_{1-x}P_x)_2$. *Journal of Physics: Condensed Matter* **23**, 065701 (2011).
31. Stojchevska, L. *et al.* Electron-phonon coupling and the charge gap of spin-density wave iron-pnictide materials from quasiparticle relaxation dynamics. *Phys. Rev. B* **82**, 012505 (2010).
32. Rettig, L. *et al.* Electron-phonon coupling in 122 Fe pnictides analyzed by femtosecond time-resolved photoemission. *New Journal of Physics* **15**, 083023 (2013).
33. Wu, D. *et al.* Effects of magnetic ordering on dynamical conductivity: Optical investigations of $EuFe_2As_2$ single crystals. *Phys. Rev. B* **79**, 155103 (2009).
34. Hansteen, F., Kimel, A., Kirilyuk, A. & Rasing, T. Femtosecond photomagnetic switching of spins in ferrimagnetic garnet films. *Phys. Rev. Lett.* **95**, 047402 (2005).
35. Kalashnikova, A. M. *et al.* Impulsive excitation of coherent magnons and phonons by subpicosecond laser pulses in the weak ferromagnet $FeBO_3$. *Phys. Rev. B* **78**, 104301 (2008).
36. Cooper, B. R. & Elliott, R. J. Spin-wave theory of magnetic resonance in spiral spin structures: Effect of an applied field. *Phys. Rev.* **131**, 1043–1056 (1963).
37. Subkhangulov, R. *et al.* All-optical manipulation and probing of the $d - f$ exchange interaction in EuTe. *Scientific reports* **4**, 4368 (2014).
38. Iida, R. *et al.* Spectral dependence of photoinduced spin precession in $DyFeO_3$. *Phys. Rev. B* **84**, 064402 (2011).
39. Nowik, I., Felner, I., Ren, Z., Cao, G. H. & Xu, Z. A. ^{57}Fe and ^{151}Eu Mössbauer spectroscopy and magnetization studies of $Eu(Fe_{0.89}Co_{0.11})_2As_2$ and $Eu(Fe_{0.9}Ni_{0.1})_2As_2$. *New Journal of Physics* **13**, 023033 (2011).
40. Jiao, W.-H. *et al.* Anisotropic superconductivity in $Eu(Fe_{0.75}Ru_{0.25})_2As_2$ ferromagnetic superconductor. *EPL (Europhysics Letters)* **95**, 67007 (2011).

Acknowledgments

Work at Jozef Stefan Institute was supported by ARRS (Grant No. P1-0040). Work done in Zhejiang University was supported by NSFC (Grant No. 11190023).

Author contributions

T.M. conceived the idea and experiment, A.P. performed optical measurements, N.V. built broadband optical setup, G.C. and Z.-A.X. grew and characterized single crystals, T.M. and A.P. analyzed the data, T.M., A.P. and D.M. wrote the paper.

Additional information

Supplementary information accompanies this paper at http://www.nature.com/scientificreports

Competing financial interests: The authors declare no competing financial interests.

How to cite this article: Pogrebna, A. *et al.* Coexistence of ferromagnetism and superconductivity in iron based pnictides: a time resolved magnetooptical study. *Sci. Rep.* 5, 7754; DOI:10.1038/srep07754 (2015).